Journal of Catalysis 284 (2011) 34–41

Contents lists available at SciVerse ScienceDirect

Journal of Catalysis

journal homepage: www.elsevier.com/locate/jcat

# Understanding the catalytic activity of gold nanoparticles through multi-scale simulations

Simon H. Brodersen [a], Ulrik Grønbjerg [a], Britt Hvolbæk [b], Jakob Schiøtz [a,*]

[a] Danish National Research Foundation's Center for Individual Nanoparticle Functionality (CINF), Department of Physics, Building 307, Technical University of Denmark, DK-2800 Kgs. Lyngby, Denmark
[b] NanoDTU, Department of Physics, Building 307, Technical University of Denmark, DK-2800 Kgs. Lyngby, Denmark

ARTICLE INFO

*Article history:*
Received 2 June 2011
Revised 25 August 2011
Accepted 26 August 2011
Available online 5 October 2011

*Keywords:*
Gold catalysis
DFT
Monte Carlo
Multi-scale modelling

ABSTRACT

We investigate how the chemical reactivity of gold nanoparticles depends on the cluster size and shape using a combination of simulation techniques at different length scales, enabling us to model at the atomic level the shapes of clusters in the size range relevant for catalysis. The detailed atomic configuration of a nanoparticle with a given number of atoms is calculated by first finding overall cluster shapes with low energy and approximately the right size, and then using Metropolis Monte Carlo simulations to identify the detailed atomic configuration. The equilibrium number of low-coordinated active sites is found, and their reactivities are extracted from models based on Density Functional Theory calculations. This enables us to determine the chemical activity of clusters in the same range of particle sizes that is accessible experimentally. The variation of reactivity with particle size is in excellent agreement with experiments, and we conclude that the experimentally observed trends are mostly explained by the high reactivity of under-coordinated corner atoms on the gold clusters. Other effects, such as the effect of the substrate, may influence the reactivities significantly, but the presence of under-coordinated atoms is sufficient to explain the overall trend.



## 1. Introduction

Although gold is generally considered chemically inert [1], it has, since 1987, been known that gold nanoparticles can be active catalysts [2], once the particle size is reduced below 5 nm and even at temperatures as low as room temperature. The mechanism behind this has been widely debated, and no consensus has been reached. Suggestions include quantum confinement effects [3–5], charging of the nanoparticles [6–8], active participation by the support either by supplying oxygen to the cluster [9] or by the active site being localised at the interface [10–12], and the abundance of low-coordinated gold atoms on the smallest clusters [13,14]. Recent work based on Density Functional Theory (DFT) calculations combined with microkinetic models has shown that low-coordinated gold atoms at corners and possibly edges of the nanoparticles can act as active sites for catalytic CO oxidation at room temperature and that this can explain the majority of the overall trend of increased reactivity of particles smaller than 5 nm [15,16]. It should be noted that other effects, such as influence of the support, undoubtedly contribute to the reactivity, but it appears to be possible to explain the overall trend without invoking these. In a recent review, Janssens et al. [14] have compiled experimental reactivities obtained with various preparation techniques and supports and demonstrated that the overall trend is consistent with the reactivity per gram Au scaling as the particle diameter $d^{-3}$, supporting the notion of corner atoms as the main contributor to the reactivity. Overbury et al. [17] have measured the reactivity versus size for $TiO_2$-supported Au nanoparticles and found a scaling exponent between −3 and −2 depending on the loading, possibly indicating that both corner and edge atoms contribute to the reactivity.

The interpretation that corner and edge atoms are dominating the reactivity of gold nanoparticles is strongly supported by theoretical arguments. Gold surfaces do not normally bind oxygen, as the d-states of gold lie so low in energy that the interaction between the Au 5d-states and the O 2p-states is net repulsive [1]. Gold atoms situated on the edges and corners of a nanoparticle have fewer neighbouring gold atoms, which leads to a shift of the d-states to a higher energy and an increased reactivity when the reactivity is described with a simple d-band model [1,18]. Detailed calculations of the reaction path, based on DFT, have indeed confirmed this picture and shown that such under-coordinated atoms are very reactive with respect to CO oxidation [16,18].

Once this has been established, and the reactivities of typical sites have been calculated, it is in principle straightforward to calculate the reactivity of a given nanoparticle, provided the occurrences of the different sites are known. This principle has been

* Corresponding author.
*E-mail address:* schiotz@fysik.dtu.dk (J. Schiøtz).

0021-9517/$ - see front matter © 2011 Elsevier Inc. All rights reserved.
doi:10.1016/j.jcat.2011.08.016

applied to CO oxidation on gold nanoparticles [13] and also to ammonia synthesis on ruthenium nanoparticles [19]. In both cases, a relatively simple model for the particle shape was employed, based on the Wulff construction. The Wulff construction determines the thermodynamically favourable shape of crystals: the shape that minimises the surface energy for a given volume, taking the anisotropy of the surface energy into account. This is the correct approach for large particles, where the material can be considered a continuum and where the energy associated with edges and corners is negligible. However, for nanoparticles neither is the case: The excess energy associated with the atoms in the corners and edges may be comparable to the surface energies. In addition, the Wulff construction is only able to create clusters with certain "magic" numbers of atoms, corresponding to adding or removing whole atomic layers to the cluster surfaces. The Wulff construction is, therefore, only an approximation neglecting these effects. If a cluster contains a different number of atoms, it is unclear whether adding defects to a Wulff construction is going to produce a reasonable low-energy structure. As such defects consist of under-coordinated (and thus reactive) atoms, their presence or absence will dominate the reactivity of the cluster.

For the case of ruthenium clusters, Gavnholt and Schiøtz [20] have investigated the low-energy configurations of these and have found that the lowest energy configurations often depart from Wulff shapes in order to reduce the amount of corners and steps at the price of a slight increase in surface area. For the case of ammonia synthesis on ruthenium clusters, this leads to a significant reduction in available active sites compared to what would be expected from a modified Wulff construction [19]. However, these results cannot be transferred to the case of gold catalysis. The energetics of the two types of clusters differ significantly, and furthermore, the reactive site for ammonia synthesis is not a low-coordinated atoms in itself, but at the foot of an atomic step on the surfaces.

For these reasons, we are investigating the shape of gold nanoparticles, with a particular focus on the number of under-coordinated atoms as a function of particle size. An obvious approach to such a task would be molecular dynamics or Metropolis Monte Carlo simulations. However, neither of these methods is practical to apply directly to clusters containing more than a few hundred atoms, as the required simulation times would be astronomical. Instead, we introduce a two-step Monte Carlo simulation method inspired by the work of Gavnholt and Schiøtz [20]. In this method, first reasonable candidates for the overall shape of the clusters are found, followed by an investigation of the detailed shape of the clusters. The method yields an approximate Boltzmann ensemble of cluster shapes, from which the average number of under-coordinated atoms can be determined. This finally allows us to predict the overall reactivity. It should be stressed that some care is required when comparing with experimental reactivity, as we calculate the reactivity at a single size whereas experimental measurements will always involve a size distribution. Furthermore, there is no guarantee that the particles being measured upon have reached their thermodynamically most favourable state, in particular if formed at low temperature.

## 2. Method

The energy landscape of a cluster with thousands of atoms is quite complicated, with regions of many local minima separated by large energy barriers, as illustrated figuratively in Fig. 1. The close-lying minima in the figure correspond to moving individual atoms around, thus creating or removing atomic-scale defects while preserving the overall shape of the cluster. The large energy barriers illustrate moving whole layers of atoms from one side of the clusters to another, thus leading to different overall shapes of the cluster.

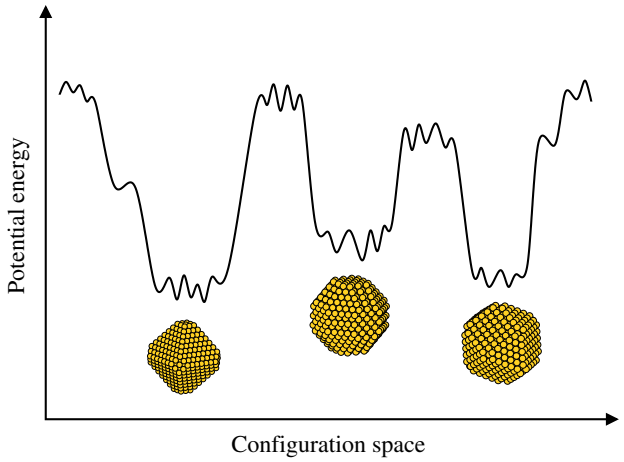


**Fig. 1.** Illustration of the energy landscape of a cluster. The large "valleys" correspond to different overall shapes of the cluster, i.e., different number of atomic layers along the various crystal directions. Within each "valley", there is a detailed structure, as in most cases the number of atoms does not correspond to all layers being perfect, and there are many possible arrangements of the few missing/additional atoms.

Any straightforward Monte Carlo algorithm based on moving individual atoms will not get past these large energy barriers. However, as the large valleys correspond to different overall cluster shapes, it is possible to sample configurational space by a two-level method. First, all the relevant "valleys" are identified by searching for reasonable overall shapes for the cluster, describing the shape with a relatively low number of parameters. A second step then investigates the detailed atomic-scale shape [20].

In the developed method, we have limited our focus to structures based on the face-centred cubic (FCC) crystal structure in order to hold the calculation time at a reasonable level. All atoms are sitting on sites belonging to an FCC lattice, we do thus not allow for defects such as stacking faults or twin boundaries, nor do we allow cluster structures that are not based on a crystal structure, such as icosahedral or decahedral clusters. However, we explicitly include the surface relaxation energies in our calculations, although technically surface relaxations correspond to the outermost atoms moving slightly away from the perfect positions.

At first sight, excluding icosahedral or decahedral clusters would seem problematic, as it is known that small metallic clusters typically have these structures, where the surface energy is minimised at the cost of slightly higher bulk energy. However, Baletto et al. [21] have investigated the crossover size between the icosahedra, decahedra and truncated octahedron (FCC) structures for different FCC metals. They find that the crossover size is strongly dependent not only on the metal studied but also on the details of the interatomic potential. Regardless of the potential, they find that gold has the strongest tendency to remain in FCC structures. When modelled with the Embedded Atom Method (which closely resembles the Effective Medium potential used here), gold prefers the FCC structure or the decahedral structure to the icosahedral structure even for the smallest clusters, whereas it is not possible to determine whether decahedral or FCC structure is preferred for clusters with less than a few hundred atoms. Other researchers find larger size ranges where the non-FCC phases are stable [22]. It would be useful to extend the method described here to explicitly include such phases; it is, however, not a trivial extension, as there is no simple underlying lattice in these phases. Furthermore, as the purpose of this work is to investigate the scaling of the reactivity with respect to the size, it is of great value to have a homogeneous

data set without sudden changes in structure, even if this means that the smallest clusters might have a structure differing from the experimentally observed structure.

For the coarse-scale simulation, we limit ourselves to structures constructed only by the low-energy (100), (110) and (111) surfaces. As an FCC crystal has six (100) directions, 12 (110) directions and eight (111) directions, a cluster can be represented by 26 integer parameters giving the distance from the centre of the cluster to these surfaces measured in atomic layers, in analogy to a Wulff construction. A Monte Carlo algorithm operating within this parameter space performs this coarse-scale search. Each Monte Carlo step starts with a random selection of a parameter, which is then increased or decreased by one, i.e., one atomic layer is either added to or removed from the surface represented by the parameter. This will change the size of the cluster, so in order to keep the size close to a specified value, another parameter is chosen randomly and then decreased or increased by one to compensate. This compensation is repeated until the size has passed the desired size leaving two configurations bracketing the correct size, which can be used as trial configurations in the Monte Carlo algorithm. Normally one would choose the configuration with the lowest energy, but the size difference makes this choice a bit blurred, so instead we chose the configuration with the lowest energy per atom. This will unfortunately favour large clusters with a high fraction of low energy bulk atoms, but at these small size differences, this is an insignificant problem. At the $n$th step, the trial configuration is accepted with the probability

$$P_{n+1} = exp\left(\frac{-\Delta E}{kT_{SMC}}\right),$$

where $\Delta E$ is the energy difference between the new and old configuration, and $T_{SMC}$ is a fictitious temperature. The energy difference is given as

$$\Delta E = (\varepsilon_{n+1} - \varepsilon_n)\frac{N_n + N_{n+1}}{2},$$

where $\varepsilon$ is the energy per atom. We scale the energies with the average size between the two clusters in order to have a temperature with physical meaning. Since this coarse-scaled simulation involves moving entire surfaces of the cluster, we shall refer to it as "Surface Monte Carlo" (SMC).

The result of the SMC simulation is an ensemble of reasonable cluster shapes, represented by defect-free clusters with sizes close to the desired number of atoms. To save computer time later, duplicates are removed by taking symmetry into account. In addition, configurations with energy more than 4 eV above the minimum energy are eliminated, as they are unlikely to contribute significantly to the final result. Each unique global cluster shape is then used as the starting point for a regular Metropolis Monte Carlo simulation in the second step of the algorithm. In this simulation, individual atoms are allowed to move to optimise the structure, for this reason we shall refer to this phase as "Atoms Monte Carlo" (AMC).

First, the number of atoms is corrected either by removing the lowest-coordinated atoms or by adding atoms to the highest-coordinated vacant sites, until the cluster has the desired size. In each step of the Monte Carlo calculation, a random surface atom is selected and moved to a random supported vacant site, i.e., a site in the FCC lattice that has at least one nearest neighbour in the cluster. At the $n$th step in the calculation, the proposed step is accepted with the probability

$$P_{n+1} = \exp\left(-\frac{E_{n+1} - E_n}{kT_{AMC}}\right).$$

Unfortunately, this acceptance probability does not fulfil the detailed balance criteria of the Metropolis Monte Carlo algorithm, because the number of available moves, and thus the probability of suggesting a given move, depends on the configuration. The variance in the available moves is, however, small and it can, therefore, be corrected *a posteriori*.

The result of the AMC simulation should be a canonical ensemble of cluster configurations corresponding to the sub-space reachable from the global cluster shape. Since each global cluster shape results in a separate atomic Monte Carlo simulation, the resulting ensembles should be combined. Unfortunately, there is no "correct" way to do this, but if we assume that the local energy landscapes around each global shape are not too different, it is a good approximation to weigh the result of each Boltzmann simulation with

$$w_s = N_s \exp\left(\frac{-E_s}{kT_{AMC}}\right),$$

where $E_s$ is the lowest energy encountered in the $s$th AMC simulation, $T_{AMC}$ is the temperature of the AMC simulations, and $N_s$ is the number of symmetrically equivalent initial cluster shapes (this factor compensates for the removal of symmetrically equivalent shapes in the coarse-grained simulation). While combining the results of the AMC simulations, we also correct the resulting ensemble for a number of phenomena, which could change it significantly. First, the energy of the cluster is calculated with all atoms in lattice sites; in reality, the surface atoms will relax inwards lowering the energy of the cluster. The relaxation energies of all clusters are calculated by minimising the energy with respect to all coordinates using the Limited-memory Broyden–Fletcher–Goldfarb–Shanno (LBFGS) algorithm [23]; the relaxed energies ($E_{relax}$) are then used to correct the ensemble. In addition, a correction factor $B_i$ compensates for the previously mentioned lack of detailed balance. Finally, it is computationally advantageous to run the AMC simulation at a higher temperature than the desired temperature ($T$); this is also corrected at this step. In summary, each configuration in the ensemble is assigned a weight

$$w_i = w_s \frac{1}{B_i}\frac{\exp(-E_{relax,i}/kT)}{\exp(-E_i/kT_{AMC})}.$$

It should be noted that the algorithm presented here differs from the algorithm suggested by Gavnholt and Schiøtz [20] in two ways. First, we allow the number of atoms in the first step to depart from the desired cluster size, whereas Gavnholt and Schiøtz already here remove or add some atoms. Secondly, we perform a full Monte Carlo simulation to find the detailed atomic-scale shapes corresponding to each global shape, whereas Gavnholt and Schiøtz attempt to sample all possible ways the atoms can be added to or removed from the global shape to give the actual cluster, reverting to a random sampling if the number of combinations is prohibitively large.

In the discussion previously, we have assumed that the energy of a cluster can be calculated. As literally millions of configurations are being examined, this must be done in a computationally efficient way. We choose to describe the energy of a gold cluster within the Effective Medium Theory (EMT) [24], as EMT has proven to give a reliable description of the noble metals. We use parameters refitted to elastic and energetic properties by Rasmussen [25,26], as these reproduce the surface energies much better than the original EMT parameters. The parameters used were $E_0 = -3.80$ eV, $s_0 = 2.60$ bohr, $V_0 = 2.703$ eV, $\eta_2 = 1.310$ bohr$^{-1}$, $\kappa = 2.757$ bohr$^{-1}$, $\lambda = 1.948$ bohr$^{-1}$, see Ref. [24] for documentation of the parameters and the functional form.

A multi-level method like this by necessity contains a number of simulation parameters that should be chosen carefully, in this case the temperatures of the SMC ($T_{SMC}$) and AMC ($T_{AMC}$) simulations, the length of the two simulations ($N_{SMC}$ and $N_{AMC}$), and the energy cut-offs ($E_{cut,AMC}$ and $E_{cut,relax}$) above which AMC is not

**Table 1**
Parameter values used in the simulations. Larger clusters require more steps in the Atomic Monte Carlo steps (but not in the Surface Monte Carlo). Furthermore, the relaxation energy increases with cluster size, and a greater cut-off is needed to insure convergence.

| Cluster size | $N_{SMC}$ | $N_{AMC}$ | $E_{cut,AMC}$ (eV) | $E_{cut,relax}$ (eV) | $T_{SMC}$ (K) | $T_{AMC}$ (K) |
|---|---|---|---|---|---|---|
| $\leqslant$1000 | $3.2 \times 10^6$ | $1.0 \times 10^6$ | 4 | 1.24 | 4000 | 1000 |
| 2500 | $3.2 \times 10^6$ | $1.0 \times 10^6$ | 4 | 3.24 | 4000 | 1000 |
| 4500 | $3.2 \times 10^6$ | $7.0 \times 10^6$ | 4 | 4.24 | 4000 | 1000 |
| 8000 | $2.4 \times 10^6$ | $1.2 \times 10^7$ | 4 | 5.24 | 4000 | 1000 |

performed and above which configurations are no longer minimised, respectively. Significant work is saved by not performing the AMC step on configurations generated by the SMC that are unlikely to contribute to the final result. Similarly, the energy minimisation step needed for the *a posteriori* correction of the ensembles produced in the AMC can be skipped if the unrelaxed energy is sufficiently high. Great care was taken to ensure that the results were insensitive to changes in $T_{SMC}$ and $T_c$ and that they were converged with respect to the other parameters, see Table 1. Convergence of the simulations was checked by comparing two or three separate simulations and was deemed sufficient when the different simulations gave the same result, i.e., when the average cluster energy was within a few tens of meV and the distribution of CN was very close. In the worst case, the reactivity varies by less than 8% between two otherwise identical simulations.

The method as described here can handle clusters up to approximately 10,000 atoms, before the computations become unwieldy. The main limitation in addition to computer time is the storage required to store all clusters that potentially need relaxation. An alternative that could be used would be to assign energies to atoms according to their nearest neighbours only and include the relaxation energy in these energies. This was the choice made by Gavnholt and Schiøtz [20], at the price of ignoring interactions between surface defects.

## 3. Results

Using the described method, we have performed simulations on gold clusters with sizes ranging from 65 to 8000 atoms. We have chosen this lower boundary, disregarding that Baletto et al. [21] have showed that gold clusters may favour the decahedra structure at sizes below 500 atoms, in order to obtain the overall trend in catalytic activity down to very small clusters based on the FCC structure. We have specified the number of atoms in our clusters, so it is not given that we will have closed shells or filled edges. This is seen in Fig. 2, showing typical configurations for a number of clusters with different sizes. The violet atom in the cluster with 340 atoms is an adatom sitting on top of a (100) surface; this is an example of a situation where complete layers are not formed.

For each cluster size, an approximate Boltzmann ensemble was obtained, from which the average number of atoms with a given coordination number (CN) was found based on a weighted average

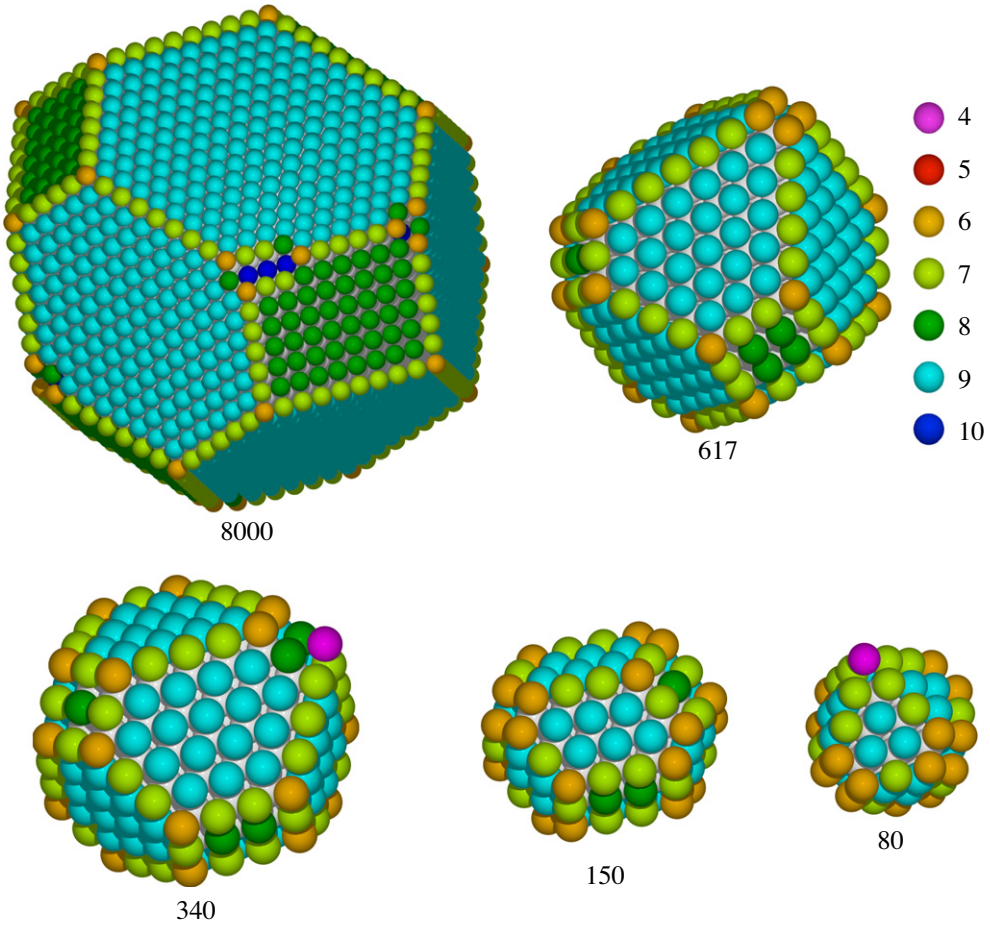


**Fig. 2.** Pictures of the configuration with lowest energy found in the simulations, for different cluster sizes. It is seen that the nine-coordinated (111) surfaces dominate the non-bulk of the clusters. When the clusters become sufficiently small, the fractions of six- and seven-coordinated corner and edge atoms become comparable to the fraction of surface atoms. Note how the clusters often can accommodate the arbitrary number of atoms by departing from Wulff-like shapes either by being elongated (the 150 atom cluster) or by breaking the symmetry between otherwise equivalent surfaces (most obvious on the 617 atom cluster, but seen on almost all clusters).

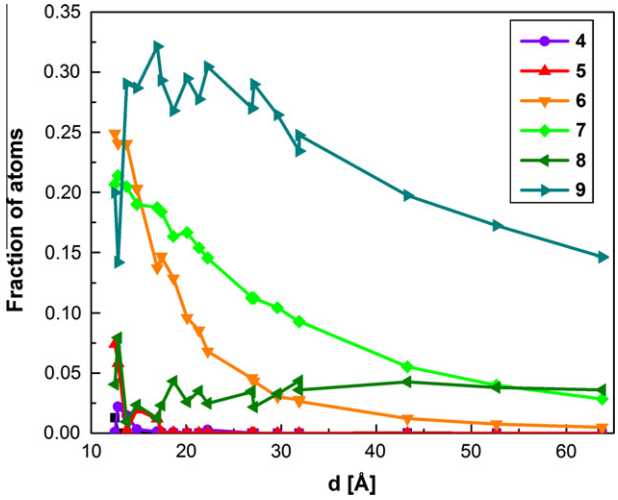


**Fig. 3.** Fraction of atoms with coordination numbers from 4 to 9.

as described in the previous section. The result can be seen in Fig. 3, where the fraction of atoms in the cluster with a CN between four and nine is plotted against the cluster diameter, which is calculated based on the volume of the atoms in the cluster assuming that the cluster is spherical. We have omitted atoms with coordination numbers below 4 or above 9, because they, respectively, are exceedingly rare or have a very small reactivity, as we will see later, and they are, therefore, of no importance to the overall reactivity.

The majority of the nine-coordinated atoms are (1 1 1) surface atoms. They are seen to dominate the non-bulk for clusters above 3 nm and their fraction is seen to increase with decreasing cluster size until 1.5 nm where it drops drastically. This drop happens because the clusters become so small that their surface is mostly made up of edges and corners instead of flat facets. The seven-coordinated atoms represent the edges between two (1 1 1) surfaces and edges between the (1 0 0) and (1 1 1) surfaces. The majority of the six-coordinated atoms are the corners between two (1 1 1) and the (1 0 0) surfaces, but six-coordinated atoms are also seen at edge defects. Both the fraction of seven- and six-coordinated atoms are seen to increase for decreasing cluster diameter as expected, where the rise for the corner atoms is steeper than the one for the edge atoms. For small clusters below 3 nm, the fraction of these atoms becomes comparable to the fraction of nine-coordinated surface atoms. The majority of the eight-coordinated atoms are mostly (1 0 0) surface atoms and their fraction is seen to be low and fairly constant, as the (1 0 0) facets are small, until the fraction begins to fluctuate for very small particles. The five-coordinated atoms are caused by defects such as vacancies at edges, and they are seen to be insignificant for clusters larger than 1.5 nm. The majority of four-coordinated atoms are corners where four (1 1 1) surfaces meet, or adatoms on (1 0 0) surface; the former can be seen as a special case of the latter where the (100) surface is only four atoms. This fraction is always small, but increases somewhat for the very smallest clusters around 1 nm. Some of these features can be seen on the five different clusters shown in Fig. 2, where the gold atoms have been colour coded according to their CN.

Based on the average number of atoms with different CN, it is straightforward to calculate the overall catalytic activity of the clusters as a function of the diameter, given that the activity per atom is known for the different CN. In previous DFT calculations, the catalytic activity of CO oxidation for the (1 1 1)- and (2 1 1)- and (5 3 2)-surfaces, with CN = 9, 7 and 6, respectively, has been calculated [18]. The activity of CO oxidation has also been found for atoms with CN 4 and 5, based on DFT calculations for a 12-atom and a 55 atom cluster, respectively [16,18]. To calculate the activity, a microkinetic model is formulated splitting the CO oxidation reaction into elementary steps. The microkinetic model is analysed using a simplified kinetic treatment, "Sabatier analysis" [27], taking into account the surface coverage and reaction rates obtained within the model with binding energies and transition barriers calculated within DFT. For all structures, 2–3 atoms are needed for the reaction, but as the reactivity is mostly determined by the coordination number of the lowest-coordinated atom, the reactivity is formally assigned to this atom. Only the dissociative oxidation path is contributing significantly to the reactivity, except for CN 4, where both the associative and dissociative mechanism are taken into account. For more details, we refer to reference 16 and 18. The resulting activities are listed in Table 2.

**Table 2**
CO and O adsorption energies on gold together with the calculated Sabatier activities and rates, where the latter is calculated at 300 K [16,18,27]. The activities are the results of using energetics calculated with DFT in a microkinetic model, as described in the references.

| CN | $E_0$ (eV) | $E_{CO}$ (eV) | $A_s$ (eV) | $r_s$ ($s^{-1}$) |
|---|---|---|---|---|
| 9 | −0.23 | 0.12 | −1.181 | $9.040 \times 10^{-8}$ |
| 7 | −0.24 | −0.23 | −0.832 | $6.593 \times 10^{-2}$ |
| 6 | −0.29 | −0.48 | −0.586 | 894.63 |
| 5 | −0.27 | −0.56 | −0.548 | 3890.6 |
| 4 | −0.59 | −0.83 | −0.529 | 8113.3 |

It should be noted that the activity of the six-coordinated atoms is around $10^4$ times larger than the one of the seven-coordinated atoms at room temperature. The activity contribution from atoms with CN larger than six is, therefore, insignificant compared to the overall activity. Furthermore, this large factor makes our results relatively insensitive to uncertainties on the calculated activities, as the main features of our results reflect the ratio of active (CN $\leqslant$ 6)-to-inactive (CN $\geqslant$ 7) atoms.

By multiplying the activity of an atom with a given CN with the fraction of atoms having this CN and sum over the CN's, we obtain the overall activity of the clusters as a function of the diameter. The result is seen in Fig. 4, where panel a show the overall activity and panel b show the activity broken up into contributions from atoms with different coordination numbers. It is important to use the Boltzmann average of the entire ensemble and not just the lowest energy cluster to find these activities, since activities calculated from the ground state configurations vary by up to 40% from the correctly calculated activities in an unsystematic way, as the presence or absence of a single defect may influence the activity significantly, and as there are often several configurations with an energy only slightly larger than the ground state.

The shape of the curve resembles the compilation of experimental data on CO oxidation on gold clusters on a variety of substrates, presented by Janssens et al. [14] The linear relationship in Fig. 4a confirms that the activity depends exponentially on the diameter of the clusters, and the exponent is found to be $-3.0 \pm 0.1$. This exponent is in excellent agreement with the expectations when corner atoms are dominating, but in less good agreement with the experimental results by Overbury et al. [17], where the exponent is found to be $-2.7 \pm 0.3$ and $-1.9 \pm 0.2$ at 298 K for two different series of gold clusters on a $TiO_2$ substrate. A scaling exponent between −2 and −3 naturally leads to the conclusion that both edge and corner sites contribute to the activity,[1] in contradiction to the DFT calculations, indicating that only corner atoms have any significant activity. However, detailed analysis of our

[1] As the number of corner atoms is independent of the particle size, the number of edge atoms scale with the diameter $d$, the number of surface atoms with $d^2$, and the total number of atoms with $d^3$, the fraction of corner and edge atoms must thus scale with $d^{-3}$ and $d^{-2}$, respectively.

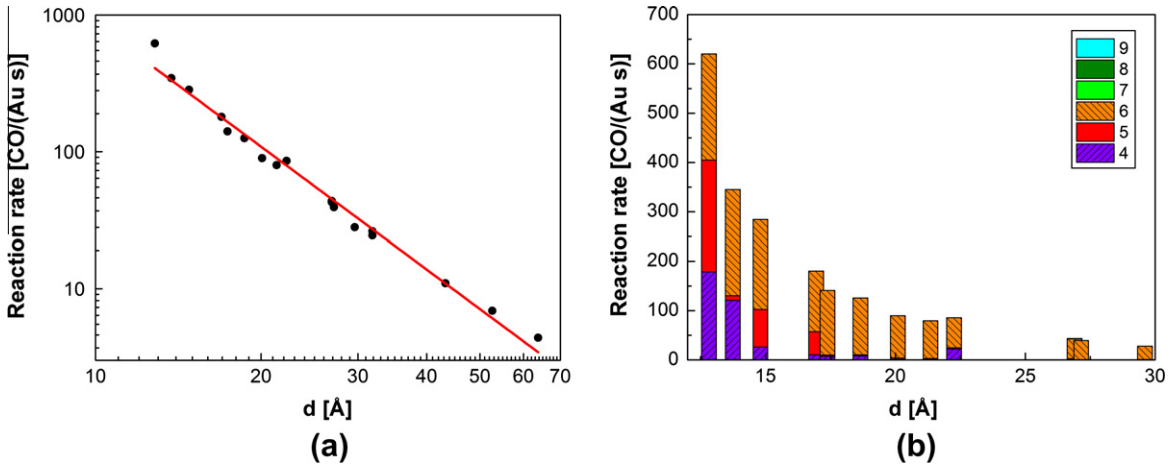


**Fig. 4.** (a) The average activities of the clusters as a function of cluster diameter on a double-logarithmic scale. The fitted line has slope −3.0 ± 0.1. In addition, the contribution to the activities from atoms with different coordination number is shown for clusters smaller than 3 nm in panel. (b) The contribution from seven- or higher coordinated atoms is negligible.

simulations indicates that corners alone may cause exponents between −2 and −3.

The experiments by Overbury et al. only address clusters larger than 2 nm; if we similarly limit our analysis to particles larger than 2 nm, we find an exponent of −2.7 ± 0.1, in perfect agreement with one of Overbury's experimental data series and consistent with the compilation of experimental reactivities by Janssen et al. This change is not random, but is caused by a small but systematic variation in the data, where the reactivity of both the smallest and largest particles are slightly above the exponential fit with slope −3.0, for two different reasons. Fig. 5 shows the absolute number of low-coordinated atoms for all the particles. It is seen that for the smallest particles, the number of six-coordinated "corner" atoms decrease, whereas a small number of five and even four coordinated atoms appear. This happens because it becomes energetically favourable to eliminate an entire (1 0 0) facet by adding a single adatom (see the 80-atom cluster in Fig. 2), effectively introducing a four-coordinated atom at the expense of four six-coordinated atoms. As the reactivity of a four-coordinated atom is more than ten times that of a six-coordinated, this actually leads to an increase in the reactivity, as we see for the very small particles.

For clusters in the range of 17–35 Å, the number of six-coordinated atoms is slightly above 24 (the number of corners in a truncated octahedron), with a weakly increasing tendency. In this size range, it is usually possible to eliminate most defects by choosing a slightly elongated cluster shape, such as the 150-atom cluster shown in Fig. 2. The increase is mostly a result of defects such as steps on the terraces, caused by the fact that the number of atoms in the clusters typically does not match the numbers one would get by making "perfect" clusters by adding whole layers to the various surfaces. With increasing cluster size, it becomes difficult to accommodate a given number of atoms in a (possibly elongated) defect-free shape without departing too much from the ideal Wulff shape, and it becomes energetically favourable to introduce a few defects, a tendency enforced by entropic effects. Again this is clearly seen in Fig. 2, most clearly for the 8000 atoms cluster. The number of corner sites is expected to grow even further for larger clusters, as the (1 1 0) facets predicted by the Wulff construction will eventually appear, leading to a doubling of the number of six-coordinated atoms. Indeed, the cluster with 4500 atoms exhibits a single (1 1 0) facet. This will lead to an exponent between −2 and −3 in this size range, as the number of corner atoms gradually increases.

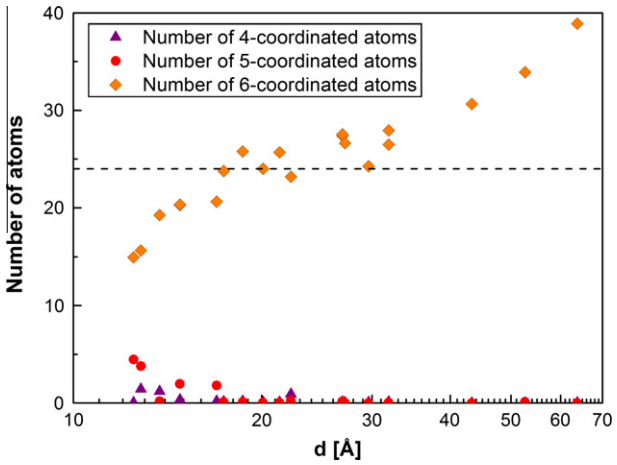


**Fig. 5.** The absolute number of low-coordinated atoms as a function of cluster size. The number of six-coordinated atoms is seen to be close to the number of corner of a truncated octahedron (24) for clusters with intermediate size, but deviates from this value for the smallest and largest clusters.

Thus, our main conclusion is that the reactivity scales as a power law with the cluster size, with an exponent between −3 and −2.7. The departure of this value from −3 is *not* caused by both edge and corner atoms contributing to the reactivity, but by corner and corner-like defect atoms alone, as is clearly seen in Fig. 4b, where the entire contribution is from atoms with coordination number six or lower. The exponent departs from −3 as it is impossible for the larger clusters to incorporate an arbitrary number of atoms in a regular, almost defect-free structure, whereas for medium-sized clusters this is often possible by producing a slightly elongated or asymmetrical cluster, as seen in Fig. 2.

## 4. Discussion

While our results are in agreement with one of the exponents found by Overbury et al. [17], when we limit our simulations to the same size range, it should be noted that they find two different exponents of −2.7 and −1.9 (at 298 K) for two differently made batches of clusters. Both batches are on $TiO_2$ substrates, but they differ in the loading of 7.2 wt.% and 4.5 wt.% gold, respectively.

Neither the experiments nor our simulations offer any explanation of this dependency on the loading, as both sets of data were taken with cluster sizes in the same range.

The measured exponents change to −2.8 and −2.1 when the temperature is lowered to 273 K. Our data are for 300 K and are thus directly comparable with Overbury's for 298 K. If we recalculate the reactivities at 273 K, it leads to a change in the exponent by −0.05 in excellent agreement with the trend seen by Overbury et al.

It should be noted that other interpretations of Overbury's measurements are possible. In a reinterpretation of Overbury's data, Bond proposes that nanoparticles below a threshold size are non-metallic and that only these are catalytically active. The power law-like dependence of reactivity with particle size would then result from the finite width of the size distribution of the clusters: with increasing average cluster size, there will be a diminishing tail of the particle size distribution reaching below the threshold size [28].

Clearly, the simulations presented here are by necessity based on a number of simplifying assumptions. As already mentioned, we assume that the overall cluster shapes are FCC-based rather than icosahedral or decahedral. While this assumption is most likely incorrect for the smallest clusters, we do not expect it to change the main result significantly, since the smallest clusters will still be able to incorporate an arbitrary number of atoms in an almost defect-free structure.

Another simplifying assumption is that we ignore interactions with the substrate. In a simple interface-energy model [29,30], interactions with the substrate will just truncate the obtained shapes, leaving all trends unaltered. However, it is likely that the role of the substrate is more complicated, as evidenced by measurements of substrate effects [9,12] and possibly by Overbury's results depending on the loading. It could be speculated that the energetics of the metal atoms sitting at the rim of the particle, where the particle surface meets the substrate, directly influences the shape of the particle; or even that these atoms are particularly reactive and participates in the reaction in a substrate-dependent way. Investigating these effects may be the topic of future work.

Finally, it should be noticed that whether the simulations of largest clusters have not been converged properly with respect to the length of the Monte Carlo simulations, the lowest energy states will not have been found, and too many defects would be observed. For this reason, special care was taken to converge the largest calculations. For the largest cluster sizes, the Monte Carlo simulations do not find the ground state, nor are they expected to do so, as the ground state will have vanishing weight in the Boltzmann ensemble. It is for this reason that the 8000-atoms cluster displays defects at more than one corner. It is, however, impossible to guarantee that the simulations have fully converged to the correct thermal distributions, in particular for the largest particle sizes. Indeed, a similar effect may influence the experiments: the largest clusters might not have completely reached the thermodynamic equilibrium shape. In both cases, this would result in a lowering of the absolute value of the exponent. One could speculate whether such effects would depend on the loading and thus contribute to the difference between the two measurement series by Overbury et al.

The two-level simulation method presented in this work brings direct simulations of cluster shapes and reactivity into a size range where the clusters can also be studied with, e.g., Transmission Electron Microscopy, thus closing the size gap between simulations and experiment. In future work, this method will most likely be extended to take into account the effects of substrate. In collaboration with experimental studies of supported catalysts, both with respect to reactivity and to cluster morphology, this may finally settle the discussion of the detailed atomic-scale mechanism of Au catalysis, including the roles of under-coordinated atoms and of the support.

## 5. Conclusion

We present a two-level Monte Carlo-based algorithm allowing us to simulate ensembles of gold clusters in the catalytically relevant size range of 1–6 nm. Our results show that the catalytic activity is entirely dominated by atoms with coordination number 6 or lower, i.e., atoms in a "corner-like" local coordination. Our results nevertheless predict a reactivity scaling with the diameter as $d^{\alpha}$ where the exponent $\alpha$ is close to −3 as expected for corner-dominated activity. However, the number of six-coordinated atoms is not fixed at 24 per cluster as would be expected from simple geometric arguments, but increases slowly for the largest clusters as defects must be incorporated into the clusters since the number of atoms rarely matches a closed-shell structure. For cluster sizes up to 4–5 nm, an arbitrary number of atoms can usually be accommodated by creating slightly skewed closed-shell clusters, but for larger clusters this becomes energetically unfavourable, defects are created and the reactivity becomes larger than otherwise expected. Alone, this would change the exponent to a value between −3 and −2, which could erroneously be interpreted as signifying that atoms at the edges contribute to the reactivity. In these simulations, this effect on the exponent is masked by a similar slight increase in reactivity of the very smallest clusters due to the appearance of four and five coordinated atoms.

Our main conclusion is that the overall trend in the size dependence of the catalytic activity of gold clusters can be explained by low-coordinated gold atoms in corner-like positions. This by no means excludes that other effects may influence the catalytic activity of gold clusters, in particular it is likely that support effects play a role, either directly by modifying the reaction at the rim of the particle or indirectly by altering the equilibrium shape of the particle. This will be the topic of further studies.

## Acknowledgments

The Center for Individual Nanoparticle Functionality (CINF) is sponsored by the Danish National Research Foundation. This work was supported by the Danish Center for Scientific Computing.

## References

[1] B. Hammer, J.K. Nørskov, Nature 376 (1995) 238–240.
[2] M. Haruta, T. Kobayashi, H. Sano, N. Yamada, Chem. Lett. 16 (1987) 405–408.
[3] Zongxian Yang, Ruqian Wu, D.W. Goodman, Phys. Rev. B (Conden. Matter Mater. Phys.) 61 (2000) 82022.
[4] X. Lai, D.W. Goodman, J. Mol. Catal. A: Chem. 162 (2000) 33–50.
[5] M. Valden, X. Lai, D.W. Goodman, Science 281 (1998) 1647–1649.
[6] G.C. Bond, D.T. Thompson, Catal. Rev. 41 (1999) 319–388.
[7] A. Sanchez, S. Abbet, U. Heiz, W.D. Schneider, H. Häkkinen, R.N. Barnett, U. Landman, J. Phys. Chem. A 103 (1999) 9573–9578.
[8] Q. Fu, H. Saltsburg, M. Flytzani-Stephanopoulos, Science 301 (2003) 935–938.
[9] M.M. Schubert, S. Hackenberg, A.C. van Veen, M. Muhler, V. Plzak, R.J. Behm, J. Catal. 197 (2001) 113–122.
[10] S. Minicò, S. Scirè, C. Crisafulli, A.M. Visco, S. Galvagno, Catal. Lett. (1997).
[11] L.M. Molina, B. Hammer, Phys. Rev. Lett. 90 (2003) 206102.
[12] G.R. Bamwenda, S. Tsubota, T. Nakamura, M. Haruta, Catal. Lett. 44 (1997) 83–87.
[13] T.V.W. Janssens, A. Carlsson, A. Puig-Molina, B.S. Clausen, J. Catal. 240 (2006) 108–113.
[14] T.V.W. Janssens, B.S. Clausen, B. Hvolbæk, H. Falsig, C.H. Christensen, T. Bligaard, J.K. Nørskov, Top. Catal. 44 (2007) 15–26.
[15] N. Lopez, T.V.W. Janssens, B.S. Clausen, Y. Xu, M. Mavrikakis, T. Bligaard, J.K. Nørskov, J. Catal. 223 (2004) 232–235.
[16] H. Falsig, B. Hvolbæk, I.S. Kristensen, T. Jiang, T. Bligaard, C.H. Christensen, J.K. Nørskov, Angew. Chem. Int. Ed. 47 (2008) 4835.
[17] S.H. Overbury, V. Schwartz, D.R. Mullim, W. Yan, S. Dai, J. Catal. 241 (2006) 56–65.
[18] T. Jiang, D.J. Mowbray, S. Dobrin, H. Falsig, B. Hvolbæk, T. Bligaard, J.K. Nørskov, J. Phys. Chem. C 113 (2009) 10548–10553.

[19] K. Honkala, A. Hellman, I.N. Remediakis, A. Logadottir, A. Carlsson, S. Dahl, C.H. Christensen, J.K. Nørskov, Science 307 (2005) 555–558.
[20] J. Gavnholt, J. Schiøtz, Phys. Rev. B 77 (2008) 035404.
[21] F. Baletto, R. Ferrando, A. Fortunelli, F. Montalenti, C. Mottet, J. Chem. Phys. 116 (2002) 3856–3863.
[22] A.S. Barnard, N.P. Young, A.I. Kirkland, M.A. van Huis, H. Xu, ACS Nano 3 (2009) 1431–1436.
[23] J. Nocedal, Math. Comput. 35 (1980) 773–782.
[24] K.W. Jacobsen, P. Stoltze, J.K. Nørskov, Surf. Sci. 366 (1996) 394–402.
[25] T. Rasmussen, Phys. Rev. B 62 (2000) 12664–12667.
[26] T. Rasmussen, private communication.
[27] T. Bligaard, J.K. Nørskov, S. Dahl, J. Matthiesen, C.H. Christensen, J. Sehested, J. Catal. 224 (2004) 206–217.
[28] G. Bond, Gold Bull. 43 (2010) 88.
[29] B.S. Clausen, J. Schiøtz, L. Gråbæk, C.V. Ovesen, K.W. Jacobsen, J.K. Nørskov, H. Topsøe, Top. Catal. 1 (1994) 367.
[30] C.V. Ovesen, B.S. Clausen, J. Schiøtz, P. Stoltze, H. Topsøe, J.K. Nørskov, J. Catal. 168 (1997) 133–142.